J. Fluid Mech. (2026), *vol.* 1034, A2, doi:10.1017/jfm.2026.11445

Is it true that no mathematical relation exists between the Navier–Stokes equations and the multifractal model?

John David Gibbon[1] and **Dario Vincenzi**[2]

[1]Department of Mathematics, Imperial College London, London SW7 2AZ, UK

[2]Université Côte d'Azur, CNRS, LJAD, Nice 06100, France

Corresponding author: John David Gibbon, j.d.gibbon@ic.ac.uk

(Received 17 November 2025; revised 3 March 2026; accepted 15 March 2026)

Contrary to accepted turbulence folklore, which holds that no mathematical relation exists between the Navier–Stokes equations (NSEs) and the multifractal model (MFM) of Parisi and Frisch, we develop a theory that reconciles the MFM with Leray's weak solutions of Navier–Stokes analysis. From a combination of Euler invariant scaling and the NSEs set in a three-dimensional box of side L, we also derive the Paladin–Vulpiani scale $\eta_{h,pav}$ which is related to the Reynolds number Re by $L\eta_{h,pav}^{-1} = Re^{1/(1+h)}$, and which acts as a mediator between the two theories. This is achieved by considering L^{2m}-norms of the velocity gradient to find a correspondence between m and the local scaling exponent h in the multifractal model. The parameter m acts as if it were the sliding focus control on a telescope which allows us to zoom in and out on different structures. The range $1 \leqslant m \leqslant \infty$ is equivalent to $-2/3 \leqslant h_{min} \leqslant 1/3$, which lies precisely in the region where Bandak *et al.* (*Phys. Rev. E*, 2022, vol. 105, p. 065113; *Phys. Rev. Lett.*, 2024, vol. 132, p. 104002) have suggested that thermal noise makes the NSEs inadequate and generates spontaneous stochasticity. The implications of this are discussed.

Key words: intermittency, fractals, Navier-Stokes equations

1. Introduction

1.1. *Historical perspective*

The language of fractal physics has been particularly useful in understanding high Reynolds number flow visualisations that show the simultaneous existence and dynamic evolution of vortical structures ranging from fully three-dimensional large vortices, down to quasi-one-dimensional filaments and even broken structures whose dimensions are less than unity. Many historical references can be found in Yeung & Ravikumar (2020), Sreenivasan & Yakhot (2021) and Jiménez (2025); see also Sreenisvasan (1991), Ishihara *et al.* (2009), Pandit *et al.* (2009), Vassilicos (2015), Yeung *et al.* (2018), Dubrulle (2019); Buaria *et al.* (2019, 2020), Elsinga *et al.* (2020, 2023), Benzi & Toschi (2023), McKeown *et al.* (2023), Mukherjee *et al.* (2024), Brewer *et al.* (2025) and Kerr (2025). In their recent report on an extensive series of $32,768^3$ computations, Yeung *et al.* (2025) have pointed out that

> *Three-dimensional turbulence governed by the Navier–Stokes equations continues to be a grand challenge in computational science, even as leadership-class computing power has recently advanced past exascale.*

Theoretical approaches involving fractal geometry and dynamical systems began to intersect in the 1970s and 1980s when conventional descriptions of fluid turbulence as merely quasiperiodic motion (Landau & Lifshitz 1959) began to be questioned: see the history described by Ruelle (1995). In their influential paper, Ruelle & Takens (1971) suggested that, as the Reynolds number increased, fluid motion would pass through a generic sequence of bifurcations, which included both periodic and quasi-periodic motion, but whose end state was chaotic motion on a strange attractor. This end state was interpreted as 'turbulence', although it is now recognised that this specific sequence is only applicable to tightly confined low-dimensional dynamical systems: see the review by Eckmann (1981) and the paper by Libchaber & Maurer (1982). The applicability of these ideas to the Navier–Stokes equations (NSEs) lay open to question because the theory expounded by Ruelle (1978*a*,*b*) was valid for finite-dimensional dissipative dynamical systems. The subsequent proof by Foias & Temam (1979) that the two-dimensional (2-D) NSEs possess a finite-dimensional global attractor $\mathcal{A}$ made the connection secure in this case. Indeed, the further work by Ruelle (1982), Constantin & Foias (1985) and Constantin (1987) on Lyapunov exponents of $\mathcal{A}$ laid the basis for the sharp (to within logarithms) estimate of the Lyapunov dimension of the 2-D Navier–Stokes global attractor (Constantin, Foias & Temam 1988). It must be stressed, however, that this process cannot be followed through for the 3-D NSEs. The Millenium problem of the global regularity of solutions in three dimensions remains open and therefore the existence of a finite-dimensional global attractor remains open. What is known rigorously is the existence of Leray–Hopf weak solutions (Leray 1934; Hopf 1951), and it is the correspondence between these and the multifractal model which is the topic of this paper.

The wide range of scales observed in turbulent flows has traditionally been interpreted in terms of a Richardson cascade which involves the transfer of energy from large to smaller scales of motion: see Monin & Yaglom (1975) and also the review by Jiménez (2000) who have discussed the effect of intermittency on cascades. Mandelbrot (1977) popularised the idea that this wide range of scales indicates an underlying fractal geometric structure, but it also became increasingly clear that the idea of a monofractal system with just a single dimension was not enough to provide an adequate description. Parisi & Frisch (1985) then interpreted these cascade processes in multifractal terms where there is a continuous spectrum of dimensions. A parameter designated as h, which appears naturally in the invariant scaling of the underlying Euler equations (see (1.3)), was used as a local scaling exponent, with each value of h belonging to a given fractal set of dimension $D(h)$. This has become known as the multi-fractal model (MFM) of turbulence: expositions can be found in Meneveau & Sreenivasan (1991), Frisch (1995), Bohr *et al.* (1998), Boffetta *et al.*

(2008), Benzi & Biferale (2009) and Frisch (2016), together with two series of lecture notes by Eyink (2008) and Benzi & Toschi (2023). In fact, multifractal scaling has a broad application in the physical sciences (Stanley & Meakin 1988). While hydrodynamic turbulence is perhaps its most prominent example, other turbulent systems must be included, such as passive scalar fields (Prasad *et al.* 1988) and bacterial suspensions (Liu & Lin 2012).

1.2. *A reconciliation between the MFM and the NSEs*

It has become part of the folklore of turbulence that no mathematical relation exists between the MFM, which is applicable to statistically steady, homogeneous, isotropic turbulence (HIT), and the forced incompressible 3-D NSEs

$$(\partial_t + \boldsymbol{u}\cdot\nabla)\,\boldsymbol{u} + \nabla p = \nu\Delta\boldsymbol{u} + \boldsymbol{f}(\boldsymbol{x}) \quad \operatorname{div}\boldsymbol{u} = 0, \tag{1.1}$$

which are evolution equations requiring specific initial conditions. In (1.1) $\boldsymbol{u}$, p and ν are respectively the velocity field, pressure and viscosity of the fluid, while $\boldsymbol{f}(\boldsymbol{x})$ is the body forcing. Building on piecemeal attempts in this direction (Dubrulle & Gibbon 2022; Gibbon 2023), this paper will demonstrate that a reconciliation between the two theories is possible. There are two ways of approaching this reconciliation, both of which involve a result of Paladin & Vulpiani (1987*a*,*b*) who used the MFM formalism to introduce a length scale into Navier–Stokes turbulence, which we call the PaV scale $\eta_{h,pav}$ (to avoid confusion with potential vorticity). In terms of the Reynolds number *Re* the inverse PaV scale is

$$\ell\eta_{h,pav}^{-1} = Re^{1/(1+h)}, \tag{1.2}$$

where the definition of the Reynolds number in Paladin & Vulpiani (1987*a*,*b*) was originally based on the energy dissipation rate and was derived using phenomenological arguments rather than directly from the NSEs. Moreover, the velocity field was assumed to be statistically stationary. To establish a mathematical relation between the MFM and the NSEs, it is critical that we use a definition of the PaV scale that is not only based on the NSEs but which is also expressed in terms of a NS-based Reynolds number. Let us consider the invariant scaling of the Euler equations. Let η be an inner length scale $0 < \eta \leqslant \ell$ and ℓ an outer scale which, in the periodic case, would be the box size $\ell = L$. Consider the incompressible Euler equations in dimensional variables $\boldsymbol{u}(\boldsymbol{x},\ t)$. If we introduce a typical velocity U_0, a frequency $\varpi_0 = U_0\ell^{-1}$ and the dimensionless parameter $\lambda = \ell\eta^{-1} \geqslant 1$, then the dimensionless set of primed variables $\boldsymbol{u}'(\boldsymbol{x}',\ t')$ defined by $(h + 1 > 0)$

$$\boldsymbol{x}' = \lambda\ell^{-1}\boldsymbol{x}, \quad t' = \lambda^{1-h}\varpi_0 t, \quad \boldsymbol{u} = U_0\lambda^{-h}\boldsymbol{u}', \tag{1.3}$$

transforms the Euler equations in dimensional variables into the dimensionless Euler equations in primed variables. While the Euler equations are invariant under the transformation in (1.3) for every value of $\lambda \geqslant 1$, the NSEs are not. Instead, direct application of (1.3) to the NSEs (1.1) shows that $\eta = \eta_{h,pav}$ is that particular value of η for which the NSEs in dimensional variables $\boldsymbol{u}(\boldsymbol{x},\ t)$ and with corresponding Reynolds number $Re = \ell U_0\nu^{-1}$, are transformed into the NSEs in dimensionless variables $\boldsymbol{u}'(\boldsymbol{x}',\ t')$ with Reynolds number equal to unity

$$\left(\partial_{t'} + \boldsymbol{u}'\cdot\nabla'\right)\boldsymbol{u}' + \nabla' p' = \Delta'\boldsymbol{u}' + \boldsymbol{f}'(\boldsymbol{x}') \quad \operatorname{div}'\boldsymbol{u}' = 0. \tag{1.4}$$

Thus, $\eta = \eta_{h,pav}$ occurs exactly where the inertial and dissipative terms balance. This interpretation of $\eta_{h,pav}$ has been used, in particular, to obtain 'fusion rules' for the statistical correlations between the inertial-range increments and the derivatives of the velocity (Benzi *et al.* 1998; Friedrich *et al.* 2018). Depending on the allowed range of h we see that the invariant scaling transformation of the Euler equations lies behind the onset of NS-turbulence as a multi-scale phenomenon. Kolmogorov's theory (Frisch 1995), known as K41, restricts this to a single scale by insisting on $h = 1/3$ but, as we see below, the MFM allows a wider spread of h. Moreover, we shall also see that the PaV scale is much more than just a bridge between the Euler and the NSEs because it also stitches together the MFM and Leray's weak solution formalism of the NSEs (Leray 1934; Robinson *et al.* 2016) which is manifest as sequences of bounded time averages (Gibbon 2019, 2020).

Our first approach, expounded in § 4.1, is to adapt the method of Dubrulle & Gibbon (2022) for evaluating the higher norms of the velocity gradient by using the Euler scaling invariance in the probabilistic sense of the MFM at the wavenumber $k_{h,pav} = \eta^{-1}_{h,pav}$. Selecting only this wavenumber in the spectrum with a variation in h, and then averaging over h, circumvents the difficulty with the Kolmogorov picture where the spectrum is divided into the inertial range and the dissipation range, a division which conventional Sobolev methods of NS-analysis do not recognise. Comparison with time-averaged results from the NSEs in § 4.2 shows that the results are consistent with the four-fifths law; namely that the multifractal spectrum (co-dimension) obeys the inequality $C(h) \geqslant 1 - 3h$, with h lying in the range $-2/3 \leqslant h \leqslant 1/3$. This corresponds to the dissipation range. The typical velocity field U_0 in (1.3) is chosen as the root-mean-square velocity field of the NSEs, as in (3.2), and the outer scale ℓ is chosen as the box scale L of the NSEs. The outer scale ℓ could equivalently be taken as the integral scale of the velocity or the characteristic length scale of the forcing. Such choices would yield an additional prefactor $(L/\ell)^3$ in the Navier–Stokes estimates provided in § 3, but would not change the way the estimates scale with *Re*, which is the key element in our analysis.

The second idea also involves the PaV scale but in the reverse order. In § 4.2 the parameter m in the L^{2m}-norms of the velocity gradient is treated as if it were the sliding focus control of a telescope through which one can zoom in and out on intermittent events. This allows us to mimic weak solution time averages as if they exist on a multifractal set $\mathbb{F}_m$ whose range of dimensions is $\mathfrak{D}_m = 3/m$. Under the assumption that the NS flow has settled into a fully developed state, $\mathfrak{D}_m$ can then be compared with $D(h)$. This gives a simple relation between the scaling exponent h and m. The range $1 \leqslant m \leqslant \infty$ corresponds to $-2/3 \leqslant h_{min} \leqslant 1/3$, which gives a cutoff deep in the dissipation range. The PaV scale $\eta_{h,pav}$ then re-emerges as the best estimate over all m for the natural length scale of the problem.

1.3. *Connection with two open questions*

The invariance of the Euler equations and their correspondence with the NSEs also touches recent work on Onsager's conjecture (Onsager 1949; Eyink 1995, 2024; Eyink & Peng 2025). De Lellis & Székelyhidi (2009, 2010) have shown that the incompressible 3-D Euler equations possess 'wild solutions' whose kinetic energy $e(t)$ does not have to be decreasing in time and may have compact support, thus suggesting a strong degree of irregularity. These solutions, found by the method of convex integration, imply that the fluid could suddenly burst into rapid motion, and then return to rest after a finite period of time. An equivalent result has been proved for the NSEs by Buckmaster & Vicol (2019, 2021). These solutions belong to the space $W^{1,1}$ for all time, which means that both $\|\boldsymbol{u}\|_1$ and $\|\nabla\boldsymbol{u}\|_1$ remain finite. However, $\|\nabla\boldsymbol{u}\|_2$ is not integrable in time so they do not satisfy a Leray–Hopf-type energy inequality. The suggestion that wild solutions may be the root cause of NS turbulence is both speculative and controversial but it is nevertheless an interesting and important open question. The magazine article by Eyink *et al.* (2025) covers a wide range of opinion by several authors over the issue of whether the Buckmaster–Vicol result is physically relevant to hydrodynamics. What is clear is that this issue has yet to be settled. A further argument is that the flaw lies in the NSEs themselves. The suggestion that thermal noise could make the deterministic version of the incompressible NSEs inadequate to describe the dissipation range of turbulence was first raised by Ruelle (1979, 1995). This is precisely the region covered by the PaV scale. More recently, Bandak *et al.* (2022, 2024) have gone further by arguing that in molecular fluids Eulerian spontaneous stochasticity (Gawędzki 2008; Thalabard *et al.* 2020) is triggered by thermal noise in 3-D Navier–Stokes turbulence at high Reynolds numbers and that this directly alters the turbulent dissipation range below the Kolmogorov scale. Bandak *et al.* (2024) conclude that the NSEs should be replaced by a Landau–Lifshitz-type set of equations which is comprised of the incompressible NSEs plus an additive fluctuating stress term proportional to div $\boldsymbol{\xi}$, where $\boldsymbol{\xi}$ is modelled as a mean-zero Gaussian random field with a given ensemble average. The range of scales over which it is conjectured that these thermal effects take place not only includes the dissipation range but also reaches into the inertial range, which illustrates why it is important that this issue is resolved. Moreover, if this argument turns out to be correct then it will change the direction of analysis in fluid dynamics. The search for a regularity proof of the 3-D deterministic NSEs, although unsuccessful, has been one of the major issues in rigorous fluid dynamics in the past generation (Leray 1934; Foias, Guillopé & Temam 1981; Robinson *et al.* 2016; Gibbon 2019). In contrast, the Landau–Lifschitz equations, having been designed as mesoscopic field equations with a high-wavenumber cutoff, have been proved to have strong, pathwise-unique solutions (Flandoli 2008; Eyink 2024).

2. The multifractal model of turbulence

The MFM is well established in the literature, so we provide only the briefest of summaries (Frisch 1995; Bohr *et al.* 1998; Boffetta *et al.* 2008; Eyink 2008; Benzi & Biferale 2009; Benzi & Toschi 2023). The pth-order longitudinal velocity structure function S_p at a point $\boldsymbol{x}$ in an HIT flow is defined as

$$S_p(r) = \left\langle \left\{ [\boldsymbol{u}(\boldsymbol{x}+\boldsymbol{r}) - \boldsymbol{u}(\boldsymbol{x})] \cdot \hat{\boldsymbol{r}} \right\}^p \right\rangle_{stat.av.}, \tag{2.1}$$

where r is the radius of the sphere centred at $\boldsymbol{x}$. While the details of the statistical average are of little concern, the scaling properties of S_p in the infinite Reynolds number limit are crucial as they revolve around the invariance property of the incompressible Euler equations. The K41 formalism assumes that S_p depends only on r and the energy dissipation rate $\varepsilon = \nu L^{-3} \int_V |\nabla \boldsymbol{u}|^2 \, \mathrm{d}V$. Since the product εr has the same units as u^3, the only scaling consistent with physical units is $S_p \sim (\varepsilon r)^{p/3}$. According to Frisch (1995), the symbol $\sim$ means 'scales like'. This agrees with the exact result $S_3 = -4\varepsilon r/5$, which is known as the four-fifths law. While the result is elegant and satisfying, experimental and numerical data indicate that S_p scales like $S_p \sim r^{\zeta_p}$, where the exponents ζ_p deviate from linear in p by lying on a concave curve that, for $p \geqslant 3$, stays below the line $p/3$, a deviation which is attributed to intermittency (Frisch 1995). To explain this, Parisi & Frisch (1985) adapted the K41 formalism by relaxing the requirement that, for small r, the velocity increment $|\boldsymbol{u}(\boldsymbol{x}+\boldsymbol{r}) - \boldsymbol{u}(\boldsymbol{x})|$ scales as r^h with $h = 1/3$. Instead, they allowed the scaling exponent h to fluctuate. They achieved this by writing down the probability of observing a given value of h at the scale r in the form

$$P_r(h) \sim r^{C(h)}, \tag{2.2}$$

where each value of h belongs to a given fractal set of dimension $D(h)$. The co-dimension $C(h)=3-D(h)$ plays the role of the multifractal spectrum in the large deviation theory version expounded by Eyink (2008). Interpreting (2.1) as an average over the probability $P_r(h)$, and by applying a steepest descent argument, one finds the following relation for the exponent ζ_p:

$$\zeta_p=\lim_{r\to 0}\left(\frac{\ln S_p}{\ln(\varepsilon r)}\right), \quad \text{where} \quad \zeta_p=\inf_h\left[hp+C(h)\right]. \tag{2.3}$$

Thus, ζ_p and $C(h)$ are connected through a Legendre transform. Note that, when $D(h)=3$, we recover the standard K41 result that $S_p\sim(\varepsilon r)^{hp}$. The four-fifths law requires $\zeta_3=1$, thus leading to inequalities for $D(h)$ and $C(h)$

$$C(h)\geqslant 1-3h \quad \Rightarrow \quad D(h)\leqslant 3h+2. \tag{2.4}$$

An alternative definition of multifractality is based on the fluctuations of energy dissipation (Meneveau & Sreenivasan 1991; Aurell *et al.* 1992; Frisch 1995). It assumes the existence of a continuous range of scaling exponents a such that the local average of the energy dissipation rate over a ball of radius r scales like r^a over a fractal set of dimension $\mathcal{F}(a)$. Kolmogorov's refined similarity hypothesis allows a connection to be established between the two definitions of multifractality; in particular, $h=a/3$ and $D(h)=\mathcal{F}(a)$ (Aurell *et al.* 1992; Frisch 1995). Finally, it is important to note that the MFM describes the scaling properties of the velocity field and the local energy dissipation but does not provide any information on the geometric structure of the flow. To see how the multifractal formalism fits with the NSEs requires an examination of the L^{2m}-norms of the velocity gradient, which we do in the next section.

3. L^{2m}-norms of the Navier–Stokes velocity gradient

The behaviour of the pointwise in time energy dissipation rate $\varepsilon=\nu L^{-3}\int_V|\nabla\boldsymbol{u}|^2\,\mathrm{d}V$ has been one of the primary goals in turbulence research (Verma 2019). Based on the ideas of Leray (1934) and Hopf (1951), the energy inequality in a 3-D periodic domain is

$$\frac{1}{2}\int_V\left(|\boldsymbol{u}(\boldsymbol{x},\ t)|^2-|\boldsymbol{u}(\boldsymbol{x},\ 0)|^2\right)\,\mathrm{d}V+\nu\int_0^t\int_V|\nabla\boldsymbol{u}(\boldsymbol{x},\ \tau)|^2\,\mathrm{d}V\,\mathrm{d}\tau\leqslant\int_0^t\int_V\boldsymbol{u}\cdot\boldsymbol{f}\,\mathrm{d}V\,\mathrm{d}\tau. \tag{3.1}$$

Note that this is an inequality, not an equality, and is valid for weak solutions of the 3-D NSEs: see also Caffarelli, Kohn & Nirenberg (1982) for a wider definition. Behind it lies a sophisticated theory of weak convergence properties that can be found in standard textbooks such as Robinson *et al.* (2016). Doering & Foias (2002) showed how to translate estimates based on the forcing $\boldsymbol{f}$ (whose L^2-norm feeds into the Grashof number Gr) into estimates based on the Reynolds number $Re=U_0L/\nu$, which is itself based on a space–time-averaged velocity field U_0, and the time-average $\langle\cdot\rangle_T$

$$U_0^2=L^{-3}\langle\|\boldsymbol{u}\|_2^2\rangle_T, \quad \text{with} \quad \langle\cdot\rangle_T=\frac{1}{T}\int_0^T\cdot\,\mathrm{d}t. \tag{3.2}$$

The Reynolds number $Re=U_0L/\nu$ has a solid basis because U_0 is bounded for all time. The time-averaged energy dissipation rate for all smooth Navier–Stokes initial conditions and square integrable forcing is (Doering & Foias 2002)

$$\langle\varepsilon\rangle_T=\nu L^{-3}\left\langle\int_V|\nabla\boldsymbol{u}|^2\,\mathrm{d}V\right\rangle_T\leqslant L^{-4}\nu^3Re^3. \tag{3.3}$$

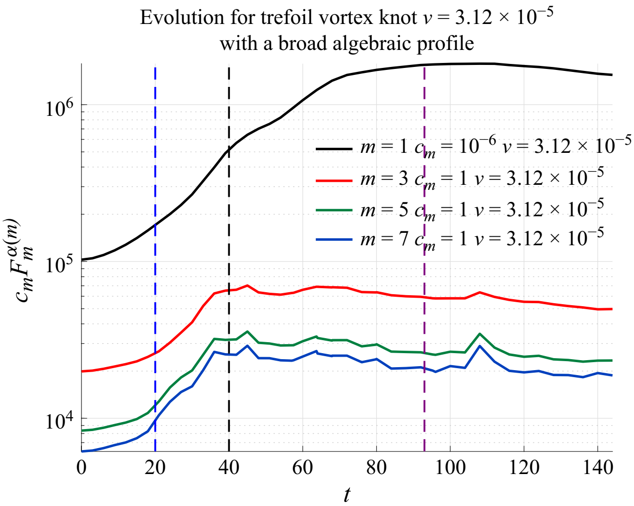

Figure 1. From the evolution of a trefoil vortex knot for $\nu = 3.12 \times 10^{-5}$, evidence appears of intermittent events at $t \approx 110$ for $m \geqslant 5$; courtesy of R. M. Kerr (2025). The vertical axis is $F_m^{\alpha_m}$ defined in (3.7) for $d = 3$ which represent scaled L^{2m}-norms of the velocity gradient.

Inequality (3.3) leads to the standard inverse Kolmogorov length estimate $L\lambda_k^{-1} \leqslant Re^{3/4}$, consistent with K41. However, it does not take account of strong intermittent events that are washed over by the spatial L^2 average in (3.3). To address this issue we require higher L^{2m}-norms of the velocity gradient tensor

$$\|\nabla \boldsymbol{u}\|_{2m} \equiv \left(\int_V |\nabla \boldsymbol{u}|^{2m}\,\mathrm{d}V\right)^{1/2m}, \qquad 1 \leqslant m \leqslant \infty. \tag{3.4}$$

For values of m near unity the integral is insensitive to strong intermittent events: the near L^2 spatial average washes over the most intense regions of $\nabla \boldsymbol{u}$ with relatively little effect – see figure 1. However, as the value of m is raised, regions of greater intensity begin to dominate, and eventually at $m = \infty$ the most intense point of all completely dominates the integral

$$\begin{array}{ll} m = 1 & \text{corresponds to a root-mean-square average,} \\ m \text{ finite but large} & \text{corresponds to the more intense structures,} \\ m = \infty & \text{corresponds to the most intense point.} \end{array} \tag{3.5}$$

Thus, the sliding scale of $m = 1 \to \infty$ acts as a zoom lens of a telescope. To find time averages of $\|\nabla \boldsymbol{u}\|_{2m}$ for $m \geqslant 1$ first requires a result of Foias, Guillopé & Temam (1981), which deserves to be better known, and which is based around nth-order weak derivatives within the volume integrals $H_n = \int_V |\nabla^n \boldsymbol{u}|^2\,\mathrm{d}V$. The Foias, Guillopé & Temam (1981) result is that Leray's weak solutions satisfy

$$\left\langle H_n^{\frac{1}{2n-1}} \right\rangle_T \leqslant c\, L^{-1} \nu^{\frac{2}{2n-1}} Re^3 + O\left(T^{-1}\right), \tag{3.6}$$

in which the energy inequality is simply the case $n = 1$. Using the Doering & Foias (2002) method, the estimate has been translated into the Reynolds number Re. Interpolation inequalities, together with (3.6), can then easily be used to find time averages of certain powers of $\|\nabla^n \boldsymbol{u}\|_{2m}$. Generalising to other spatial dimensions $d = 1, 2, 3$, these results can be rolled into a single formula (Gibbon 2019, 2020, 2023). While $n \geqslant 3$ spatial

https://doi.org/10.1017/jfm.2026.11445 Published online by Cambridge University Press

derivatives in (3.6) are necessary for the proof, once this has been achieved, all we need are estimates of time averages of powers of the single derivative $\|\nabla \boldsymbol{u}\|_{2m}$ written as two simple dimensionless formulas

$$F_{m,d} = \nu^{-1} L^{1/\alpha_{m,d}} \|\nabla \boldsymbol{u}\|_{2m}, \quad \alpha_{m,d} = \frac{2m}{4m-d}, \tag{3.7}$$

where all the results rolled together can be summarised in the formula

$$\left\langle F_{m,d}^{(4-d)\alpha_{m,d}} \right\rangle_T \leqslant c_m Re^3. \tag{3.8}$$

This, then, is the dimensionless generalisation of (3.3) to values $m \geqslant 1$ and d dimensions. Note that when $m = 1$, the factor of $4-d$ cancels and we recover the result on the energy dissipation rate in (3.3). This result is the key not only to the correspondence between the MFM and the NSEs but also the PaV scale. Donzis *et al.* (2014) studied the evolution of $\|\boldsymbol{\omega}\|_{2m}$ numerically for 4 different data sets. for values $m = 1, \ldots, 9$. Figure 1 is a plot of $F_{m,3}^{\alpha_{m,3}}$ from Kerr (2025) (courtesy of R.M. Kerr) similar to its equivalent in Donzis *et al.* (2014). The subscript $d = 3$ has been suppressed. The bound in (3.8) is a rigorous Navier–Stokes result. In the next section, we will show how it can be used in connection with the phenomenological predictions of the MFM to reconcile the two approaches.

4. Two ways of reconciling the MFM and the NSEs

4.1. *The PaV scale as a mediator between the MFM and the NSEs*

Having seen the properties of the Euler invariant scaling transformation in § 1, it is now time to apply this to the L^{2m}-norms of the velocity gradient defined in (3.4). To find a way around the problem of how to match results from the MFM with those from the NSEs, we adapt the method outlined in Dubrulle & Gibbon (2022) where only the wavenumber $k_{h,pav}$ out of all possible wavenumbers was chosen, with a subsequent integration over h. Instead, by using the scaling transformation (1.3) on the energy dissipation rate, we keep all wavenumbers but select the PaV scale $k_{h,pav} = \eta_{h,pav}^{-1}$ as the only one with h-dependence, where the probability of observing a given exponent h at the scale η is $P_\eta(h)$. We adapt (2.2) to make it non-dimensional so that

$$P_\eta(h) \sim \left[L^{-1}\eta\right]^{C(h)}, \tag{4.1}$$

where each value of h belongs to a given fractal set of dimension $D(h) = 3 - C(h)$. Our strategy is to calculate the MFM equivalent of (3.8) and compare the *Re*-scaling in the two formulations. This requires the application of the rescaling in (1.3) and an average over h to obtain

$$\frac{\int_V |\nabla \boldsymbol{u}|^{2m}\, \mathrm{d}V}{\int_V \mathrm{d}V} = U_0^{2m} \left[\int_{h_{min}}^{h_{max}} P_\eta(h) \eta^{-2m} (L\eta^{-1})^{-2mh}\, \mathrm{d}h\right] \frac{\int_{V'} |\nabla' \boldsymbol{u}'|^{2m}\, \mathrm{d}V'}{\int_{V'} \mathrm{d}V'}, \tag{4.2}$$

in which case the $F_{m,3}$ in (3.7) for $d = 3$ becomes

$$\begin{aligned} F_{m,3} &= \nu^{-1} L^{1/\alpha_{m,3}} \|\nabla \boldsymbol{u}\|_{2m} \\ &\sim \nu^{-1} U_0 L \left[\int_{h_{min}}^{h_{max}} \left(L^{-1}\eta\right)^{C(h)} (L\eta^{-1})^{2m(1-h)}\, \mathrm{d}h\right]^{1/2m} \left(\frac{\int_{V'} |\nabla' \boldsymbol{u}'|^{2m}\, \mathrm{d}V'}{\int_{V'} \mathrm{d}V'}\right)^{1/2m}. \end{aligned} \tag{4.3}$$

Now we use the PaV scale $L\eta_{h,pav}^{-1} = Re^{1/(1+h)}$ to obtain

$$F_{m,3} \sim Re \left[\int_{h_{min}}^{h_{max}} Re^{\frac{2m(1-h)-C(h)}{1+h}} \,\mathrm{d}h \right]^{1/2m} \left(\frac{\int_{V'} |\nabla' \boldsymbol{u}'|^{2m} \,\mathrm{d}V'}{\int_{V'} \mathrm{d}V'} \right)^{1/2m}. \tag{4.4}$$

In the primed variables in (4.4), the equivalent Reynolds number is unity when $k_{h,pav} = \eta_{h,pav}^{-1}$ so this term is not a function of Re. Therefore, in the limit $Re \to \infty$, by approximating the integral over h by a steepest descent argument and matching the exponents of Re on the left-hand side with Re^3 on the right from (3.8), we must have

$$\alpha_{m,3} \left[1 + \max_h \left(\frac{2m(1-h) - C(h)}{2m(1+h)} \right) \right] \leqslant 3, \tag{4.5}$$

in which case

$$\min_h C(h) \geqslant 4m\,[1 - 3(1+h)] + 9(1+h). \tag{4.6}$$

The first term on the right-hand side of (4.6) must be negative to avoid $C \to \infty$ as $m \to \infty$, thus restricting h to the range $h \geqslant -2/3$. Under this restriction on h we need to maximise the lower bound on $C(h)$ with respect to m, which occurs when $m = 1$. Therefore, uniform in m, we find that

$$C(h) \geqslant 1 - 3h \quad \text{and} \quad h \geqslant -2/3. \tag{4.7}$$

This is consistent with the results of the four-fifths law in § 2 and the range of h in (4.15).

The formula in d dimensions in (3.8) incorporates a factor $4-d$ in the exponent of $F_{m,d}$ with $\alpha_{m,d} = 2m/(4m-d)$. Therefore (4.6) is replaced by

$$C(h) \geqslant 4m \left[1 - \frac{3(1+h)}{4-d} \right] + \frac{3d(1+h)}{4-d}, \tag{4.8}$$

in which case we require $h \geqslant (1-d)/3$ to prevent $C \to \infty$ as $m \to \infty$. Again, we must have $C(h) \geqslant 1 - 3h$.

4.2. *A multifractal interpretation and the re-emergence of the PaV scale*

We have now reached the point where we need to find a correspondence between the NSEs and the MFM. This only makes physical sense if a Navier–Stokes flow has become fully developed at large enough T in the same way that Eswaran & Pope (1988) showed that the negative velocity derivative skewness must have reached a certain critical level.

As mentioned in § 2, the multifractal formalism based on dissipation postulates the existence of fractal sets in each of which the local energy dissipation rate is scale invariant. This fact suggests a multifractal interpretation of the results from NS-analysis. Consider $\alpha_{m,d}$, defined in (3.7) as $\alpha_{m,d} = 2m/(4m-d)$. If we simply divide through by m we obtain a modified version of α, namely $\alpha_{1,\mathfrak{D}_m}$

$$\alpha_{m,d} = \frac{2m}{4m-d} = \frac{2}{4-\mathfrak{D}_m} = \alpha_{1,\mathfrak{D}_m}, \quad \text{where} \quad \mathfrak{D}_m = d/m, \tag{4.9}$$

where the domain dimension d has been replaced by $\mathfrak{D}_m$. This means that working in the space $L^{2m}(\mathcal{V})$ in d dimensions can be mimicked by working in the space $L^2(\mathbb{F}_m)$ in $\mathfrak{D}_m$ dimensions. We can therefore think of $\mathbb{F}_m$ as a fractal set with a range of dimensions $\mathfrak{D}_m$. Moreover, we can rewrite the exponent $(4-d)\alpha_{m,d}$ in (3.8) with d replaced by $\mathfrak{D}_m$

$$(4 - \mathfrak{D}_m)\alpha_{1,\mathfrak{D}_m} = 2. \tag{4.10}$$

This suggests that, instead of writing down ε in L^2 for $d=3$ as in (1.1), we define a set of dissipation rates $\{\varepsilon_m\}$

$$\varepsilon_m = \nu L^{-\mathfrak{D}_m} \left\langle \int_{\mathbb{F}_m} |\nabla \boldsymbol{u}|^2 \,\mathrm{d}V \right\rangle_T, \quad \mathfrak{D}_m = 3/m \tag{4.11}$$

for each value of m, on the fractal set $\mathbb{F}_m$. This latter may be regarded as the set in which the energy dissipation rate averaged over a ball of radius r scales like r^{a_m}, although the dependence of the scaling exponent a_m on m remains unknown. Moreover, to obtain the full dissipation rate requires a measure over which to sum m, but so far this has eluded us. Noting that $\mathbb{F}_m \subset \mathbb{T}^3$, (4.11) can be re-written as

$$\varepsilon_m \leqslant \nu L^{3-\mathfrak{D}_m} \left\langle L^{-3} \int_{\mathbb{T}^3} |\nabla \boldsymbol{u}|^2 \,\mathrm{d}V \right\rangle_T \leqslant c\, L^{-1-\mathfrak{D}_m} \nu^3 Re^3. \tag{4.12}$$

Aurell *et al.* (1992) wrote down the formula (4.12) but with an arbitrary fractal dimension D whereas, for each m, here we have a fractal set $\mathbb{F}_m$ with a dimension $\mathfrak{D}_m$ that is directly associated with the NSEs. Furthermore $\varepsilon_m \nu^{-3}$ can be expressed in terms of a set of inverse lengths η_m^{-1} defined such that

$$\varepsilon_m \nu^{-3} := \eta_m^{-1-\mathfrak{D}_m} \quad \Rightarrow \quad L\eta_m^{-1} \leqslant c\, Re^{\frac{3}{1+\mathfrak{D}_m}}. \tag{4.13}$$

Note that when $\mathfrak{D}_1 = 3$ we recover the Kolmogorov estimate $Re^{3/4}$ with a continuum of values up to Re^3 for $\mathfrak{D}_\infty = 0$.

If $\mathfrak{D}_m$ is interpreted as the dimension of the set $\mathbb{F}_m$ in which the local energy dissipation rate scales as r^{a_m}, it now seems natural to equate $\mathfrak{D}_m$ in (4.11) to the fractal dimension $\mathcal{F}(a_m)$ and therefore to $D(h)$. Inequality (2.4) leads to a simple inequality relating m and h

$$\frac{3}{m} \leqslant 2 + 3h. \tag{4.14}$$

We find $h \geqslant h_{min}$ with $h_{min} = m^{-1} - 2/3$. The two limits $m \to 1$ and $m \to \infty$ give

$$-2/3 \leqslant h_{min} \leqslant 1/3. \tag{4.15}$$

Thus h is bounded away from $h=-1$. Using the inequality relation between h and m we can bound the exponent $3/(1+\mathfrak{D}_m)$ in (4.13) by

$$\frac{1}{1+h} \leqslant \frac{3}{1+\mathfrak{D}_m}. \tag{4.16}$$

The PaV inverse scale $\eta_{h,pav}^{-1}$ thus emerges as the minimiser of the right-hand side for all m. The left-hand side of (4.16) is derived directly from the MFM, while the right-hand side comes from the NSEs. In (4.15), $h_{min} \geqslant -2/3$ bounds h away from the dangerous value of $h=-1$, where a singularity can occur. The limit $h_{min} = -2/3$ corresponds to $\mathfrak{D}_m = 0$.

5. Conclusion: Is our understanding of the dissipation range correct?

The PaV length scale $\eta_{h,pav}$ is that value of η in the invariant transformation of the Euler equations which, when applied to the NSEs, gives unit Reynolds number, thus implying that the inertial and dissipation terms balance. Figure 2 shows the inter-relation between the Euler equations, the NSEs, the MFM and the central intermediary role of $\eta_{h,pav}$. One of the difficulties of making a comparison between the MFM, applicable to statistically steady HIT, and the dynamic NSEs is that the weak solution methods devised by Leray

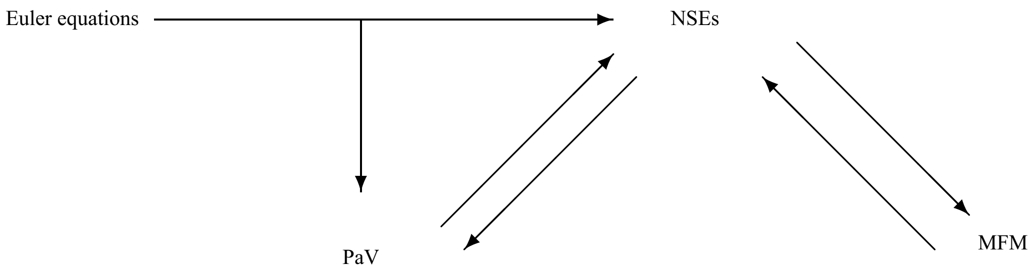

Figure 2. Pictorial representation of how the PaV scale appears as a mediator between the Euler and NSEs. Following the arrows: (i) clockwise: application of the PaV scale to the NSEs implies results consistent with the MFM; (ii) anti-clockwise: the MFM and NSEs together imply the PaV scale.

(1934) do not readily recognise a distinction between the inertial and dissipation ranges. Using the PaV scale $\eta_{h,pav}$ solves this difficulty by choosing $k = k_{h,pav}$ as the only value in the spectrum that is allowed to be h-dependent. In effect, this process auto-selects the dissipation range only. Taking the probability of observing a given scaling exponent h at the scale η to be $P_\eta(h) \sim \eta^{C(h)}$, where each value of h belongs to a given fractal set of dimension $D(h)$, it is shown in § 4.1 that a consequence of Leray's weak solution estimates leads to the inequality $C(h) \geqslant 1 - 3h$, which is consistent with the four-fifths law. It is also shown in § 3 that the parameter m in the L^{2m}-norms of the velocity gradient acts as a zoom lens focus control which is related to h.

The standard picture from large-scale computational fluid dynamics (CFD) is of the formation of vortical sheets, their roll-up into tubes and the breakdown of these into low-dimensional fractal segments. These sub-Kolmogorov vortical structures are usually identified with the dissipation range, in this case defined by $Lk_{h,pav} = Re^{1/(1+h)}$ with $-2/3 \leqslant h \leqslant 1/3$. In fact, the $-2/3$ lower bound on h corresponds to a Re^3 upper bound on the inverse length scale which is already close to, or deeper than, molecular scales even for modest values of Re. The inter-relation between the NSEs, the MFM and the central role of $\eta_{h,pav}$ identified in this paper is delicately balanced around the invariance of the Euler equations, a balance which could easily be overturned by other processes. If the suggestion by Bandak *et al.* (2022, 2024) is correct that the thermal noise generates spontaneous stochasticity, thereby overwhelming the dissipation range, then this points to a rethink of how high-Re small-scale turbulence ought to be considered. In turn it would also suggest a necessary revision of the standard CFD picture of low-dimensional structures associated with the dissipation range.

Acknowledgements. Thanks are due to R.M. Kerr for figure 1. The authors would also like to thank the Isaac Newton Institute for Mathematical Sciences, Cambridge, for support and hospitality during the programme 'Anti-diffusive dynamics: from sub-cellular to astrophysical scales' where work on this paper was undertaken. This work was supported by EPSRC grant no EP/R014604/1.

Declaration of interests. The authors report no conflicts of interest.

References

Aurell, E., Frisch, U., Lutsko, J. & Vergassola, M. 1992 On the multifractal properties of the energy dissipation derived from turbulence data. *J. Fluid Mech.* **238**, 467–486.

Bandak, D., Goldenfeld, N., Mailybaev, A. & Eyink, G. 2022 Dissipation-range fluid turbulence and thermal noise. *Phys. Rev. E* **105**, 065113.

Bandak, D., Mailybaev, A., Eyink, G. & Goldenfeld, N. 2024 Spontaneous stochasticity amplifies even thermal noise to the largest scales of turbulence in a few eddy turnover times. *Phys. Rev. Lett.* **132**, 104002.

BENZI, R. & BIFERALE, L. 2009 Fully developed turbulence and the multifractal conjecture. *J. Stat. Phys.* **135**, 977–990.

BENZI, R., BIFERALE, L. & TOSCHI, F. 1998 Multiscale velocity correlations in turbulence. *Phys. Rev. Lett.* **80**, 3244–3247.

BENZI, R. & TOSCHI, F. 2023 Lectures on turbulence. *Phys. Rep.* **1021**, 1–106.

BOFFETTA, G., MAZZINO, A. & VULPIANI, A. 2008 Twenty-five years of multifractals in fully developed turbulence: a tribute to Giovanni Paladin. *J. Phys. A: Math. Theor.* **41**, 363001.

BOHR, T., JENSEN, M., PALADIN, G. & VULPIANI, A. 1998 *Dynamical Systems Approach to Turbulence*. Cambridge University Press.

BREWER, W., *et al.* 2025 Intelligent sampling of extreme-scale turbulence datasets for accurate and efficient spatiotemporal model training. In *Proceedings of the SC '25 Workshops of the International Conference for High Performance Computing, Networking, Storage and Analysis*, pp. 1–10. Association for Computing Machinery.

BUARIA, D., BODENSCHATZ, E. & PUMIR, A. 2020 Vortex stretching and enstrophy production in high-*Re* turbulence. *Phys. Rev. Fluids* **5**, 104602.

BUARIA, D., PUMIR, A., BODENSCHATZ, E. & YEUNG, P.K. 2019 Extreme velocity gradients in turbulent flows. *New J. Phys.* **21**, 043004.

BUCKMASTER, T. & VICOL, V. 2019 Nonuniqueness of weak solutions to the Navier–Stokes equations. *Ann. Math.* **189**, 101–144.

BUCKMASTER, T. & VICOL, V. 2021 Convex integration constructions in hydrodynamics. *Bull. AMS* **58**, 1–44.

CAFFARELLI, L., KOHN, R. & NIRENBERG, L. 1982 Partial regularity of suitable weak solutions of the Navier–Stokes equations. *Commun. Pure Appl. Maths* **35**, 771–831.

CONSTANTIN, P. 1987 Collective L^∞ estimates for families of functions with orthonormal derivatives. *Indiana Univ. Math. J.* **36**, 603–616.

CONSTANTIN, P. & FOIAS, C. 1985 Global Lyapunov exponents, Kaplan–Yorke formulas and the dimension of the attractors for 2-D Navier–Stokes equations. *Commun. Pure Appl. Math.* **38**, 1–27.

CONSTANTIN, P., FOIAS, C. & TEMAM, R. 1988 On the dimension of the attractors in two-dimensional turbulence. *Physica D* **30**, 284–296.

DE LELLIS, C. & SZÉKELYHIDI, L. 2009 The Euler equations as a differential inclusion. *Ann. Math.* **170**, 1417–1436.

DE LELLIS, C. & SZÉKELYHIDI, L. 2010 On admissibility criteria for weak solutions of the Euler equations. *Arch. Ration. Mech. Anal.* **195**, 225–260.

DOERING, C.R. & FOIAS, C. 2002 Energy dissipation in body-forced turbulence. *J. Fluid Mech.* **467**, 289–306.

DONZIS, D.A., GIBBON, J.D., GUPTA, A., KERR, R.M., PANDIT, R. & VINCENZI, D. 2014 Vorticity moments in four numerical simulations of the 3-D Navier–Stokes equations. *J. Fluid Mech.* **732**, 316–331.

DUBRULLE, B. 2019 Beyond Kolmogorov cascades. *J. Fluid Mech.* **867**, 1–63.

DUBRULLE, B. & GIBBON, J.D. 2022 A correspondence between the multifractal model of turbulence and the Navier–Stokes equations. *Phil. Trans. R. Soc. A* **380**, 20210092.

ECKMANN, J.P. 1981 Roads to turbulence in dissipative dynamical systems. *Rev. Mod. Phys.* **53**, 643–654.

ELSINGA, G.E., ISHIHARA, T. & HUNT, J.C.R. 2020 Extreme dissipation and intermittency in turbulence at very high Reynolds numbers. *Proc. R. Soc. A* **476**, 20200591.

ELSINGA, G.E., ISHIHARA, T. & HUNT, J.C.R. 2023 Intermittency across Reynolds numbers – the influence of large-scale shear layers on the scaling of the enstrophy and dissipation in homogenous isotropic turbulence. *J. Fluid Mech.* **974**, A17.

ESWARAN, V. & POPE, S.B. 1988 An examination of forcing in direct numerical simulations of turbulence. *Comput. Fluids* **16**, 257–278.

EYINK, G.L., *et al.* 2025 Interpreting convex integration results in hydrodynamics. *EMS Maga.* **136**, 29–38.

EYINK, G. 1995 Besov spaces and the multifractal hypothesis. *J. Stat. Phys.* **78**, 353–375.

EYINK, G.L. 2008 *Turbulence Theory—Unpublished Lecture Notes Chapters 3C and 3D*. The Johns Hopkins University.

EYINK, G.L. 2024 Onsager's ideal turbulence theory. *J. Fluid Mech.* **988**, P1.

EYINK, G.L. & PENG, L. 2025 Space-time statistical solutions of the incompressible Euler equations and Landau–Lifshitz fluctuating hydrodynamics. *Nonlinearity* **38** (8), 085011.

FLANDOLI, F. 2008 An introduction to 3-D stochastic fluid dynamics. In *Stochastic Partial Differential Equations in Fluid Dynamics: Recent Progress and Prospects* (ed. S. Albeverio, F. Flandoli & Y.G. Sinai), Lecture Notes in Math. 1942, pp. 51–150. Springer.

FOIAS, C., GUILLOPÉ, C. & TEMAM, R. 1981 New a priori estimates for Navier–Stokes equations in dimension 3. *Commun. PDE* **6**, 329–359.

FOIAS, C. & TEMAM, R. 1979 Some analytic and geometric properties of the solutions of the evolution of the Navier–Stokes equations. *J. Math. Pures Appl.* **58**, 339–368.

FRIEDRICH, J., MARGAZOGLOU, G., BIFERALE, L. & GRAUER, R. 2018 Multiscale velocity correlations in turbulence and Burgers turbulence: fusion rules, Markov processes in scale, and multifractal predictions. *Phys. Rev. E* **98**, 023104.

FRISCH, U. 1995 *Turbulence: The Legacy of A. N. Kolmogorov*. Cambridge University Press.

FRISCH, U. 2016 The collective birth of multifractals. *J. Phys A: Math. Theor.* **49**, 451002.

GAWĘDZKI, K. 2008 Soluble models of turbulent transport. In *Non-Equilibrium Statistical Mechanics and Turbulence* (ed. S. Nazarenko & O.V. Zaboronski), London Mathematical Society Lecture Note Series, vol. 355. Cambridge University Press.

GIBBON, J.D. 2019 Weak and strong solutions of the 3-D Navier–Stokes equations and their relation to a chessboard of convergent inverse length scales. *J. Nonlinear Sci.* **29**, 215–228.

GIBBON, J.D. 2020 Intermittency, cascades and thin sets in three-dimensional Navier–Stokes turbulence. *EPL-Europhys. Lett.* **131**, 64001.

GIBBON, J.D. 2023 Identifying the multifractal set on which energy dissipates in a turbulent Navier–Stokes fluid. *Physica D* **445**, 133654.

HOPF, E. 1951 Über die Anfangswertaufgabe für die hydrodynamischen Glundgleichungen. *Math. Nach.* **4**, 213–231.

ISHIHARA, T., GOTOH, T. & KANEDA, Y. 2009 Study of high-Reynolds number isotropic turbulence by direct numerical simulation. *Ann. Rev. Fluid Mech.* **41**, 165–180.

JIMÉNEZ, J. 2000 Intermittency and cascades. *J. Fluid Mech.* **409**, 99–120.

JIMÉNEZ, J. 2025 Chaos, coherence and turbulence. *Phys. Rev. Fluids* **10**, 100504.

KERR, R.M. 2025 Navier–Stokes bounds and scaling for compact trefoils in large $(2\ell\pi)^3$ domains. *J. Fluid Mech.* **1025**, A3.

LANDAU, L.D. & LIFSHITZ, E.M. 1959 *Fluid Mechanics*, Course of Theoretical Physics, 1st edn., vol. 6. Pergamon Press.

LERAY, J. 1934 Sur le mouvement d'un liquide visqueux emplissant l'espace. *Acta Math.* **63**, 193–248.

LIBCHABER, A. & MAURER, J.1982 A Rayleigh Bénard Experiment: Helium in a small box. In *Proceedings NATO Advanced Summer Institute Series* (ed. T. Riste), Nonlinear Phenomena at Phase Transitions and Instabilities, vol. 77, pp. 259–286. Plenum Press.

LIU, K.-A. & LIN, I. 2012 Multifractal dynamics of turbulent flows in swimming bacterial suspensions. *Phys. Rev. E* **86**, 011924.

MANDELBROT, B. 1977 *Fractals: Form, Chance and Dimension*. Freeman.

MCKEOWN, R., PUMIR, A., RUBINSTEIN, S., BRENNER, M.P. & OSTILLA-MÓNICO, R. 2023 Energy transfer and vortex structures: visualizing the incompressible turbulent energy cascade. *New J. Phys.* **10**, 103029.

MENEVEAU, C. & SREENIVASAN, K.R. 1991 The multifractal nature of turbulent energy dissipation. *J. Fluid Mech.* **224**, 429–484.

MONIN, A.S. & YAGLOM, A.M. 1975 *Statistical Fluid Mechanics*, Mechanics of Turbulence, vol. I. MIT Press.

MUKHERJEE, S., MURUGAN, S.D., MUKHERJEE, R. & RAY, S.S. 2024 Turbulent flows are not uniformly multifractal. *Phys. Rev. Lett.* **132**, 184002.

ONSAGER, L. 1949 Statistical hydrodynamics. *Nuovo Cimento* **6**, 279—287.

PALADIN, G. & VULPIANI, A. 1987*a* Degrees of freedom of turbulence. *Phys. Rev. A* **35**, 1971–1973.

PALADIN, G. & VULPIANI, A. 1987*b* Anomalous scaling laws in multifractal objects. *Phys. Rep.* **156**, 147–225.

PANDIT, R., PERLEKAR, P. & RAY, S.S. 2009 Statistical properties of turbulence: an overview. *Pramana – J. Phys.* **73**, 157–191.

PARISI, G. & FRISCH, U. 1985 *Turbulence and predictability in geophysical fluid dynamics*. In *Proc. Int. School of Physics "E. Fermi" 1983 Varenna, Italy* (ed. M. Ghil, R. Benzi & G. Parisi), pp. 84–87. North-Holland.

PRASAD, R.R., MENEVEAU, C. & SREENIVASAN, K. 1988 Multifractal nature of the dissipation field of passive scalars in fully turbulent flows. *Phys. Rev. Lett.* **61**, 74–77.

ROBINSON, J.C., RODRIGO, J.L. & SADOWSKI, W. 2016 *The Navier–Stokes Equations*. Cambridge University Press.

RUELLE, D. 1978*a* Dynamical systems with turbulent behavior. In *Mathematical Problems in Theoretical Physics, 80* (ed. G. Dell'Antonio, S. Doplicher & G. Jona-Lasinio), Lecture Notes in Physics, vol. 80, pp. 341–360. Springer.

RUELLE, D. 1978*b* What are the measures describing turbulence? *Suppl. Prog Theor. Phys.* **64**, 339–345.

RUELLE, D. 1979 Microscopic fluctuations and turbulence. *Phys. Letts. A* **72**, 81–82.

RUELLE, D. 1982 Large volume limit of the distribution of characteristic exponents in turbulence. *Commun. Math. Phys.* **87**, 287–302.

RUELLE, D. 1995 *Turbulence, Strange Attractors and Chaos*. World Scientific. ISBN: 981-02—2310-2.

RUELLE, D. & TAKENS, F. 1971 On the nature of turbulence. *Commun. Math. Phys.* **20**, 167–192.

SREENIVASAN, K.R. 1991 Fractals and multifractals in fluid turbulence. *Ann. Rev. Fluid Mech.* **23**, 539–604.

SREENIVASAN, K.R. & YAKHOT, V. 2021 Dynamics of three-dimensional turbulence from Navier–Stokes equations. *Phys. Rev. Fluids* **6**, 104604.

STANLEY, H.E. & MEAKIN, P. 1988 Multifractal phenomena in physics and chemistry. *Nature* **335**, 405–409.

THALABARD, S., BEC, J. & MAILYBAEV, A. 2020 From the butterfly effect to spontaneous stochasticity in singular shear flows. *Commun. Phys.* **3**, 122–130.

VASSILICOS, J.C. 2015 Dissipation in turbulent flows. *Annu. Rev. Fluid Mech.* **47**, 95–114.

VERMA, M.K. 2019 *Energy Transfer in Fluid Flows: Multiscale and Spectral Perspectives*. Cambridge University Press.

YEUNG, P.K. & RAVIKUMAR, K. 2020 Advancing understanding of turbulence through extreme-scale computation: intermittency and simulations at large problem sizes. *Phys. Rev. Fluids* **5**, 110517.

YEUNG, P.K., RAVIKUMAR, K., UMA-VAIDESWARAN, R., DOTSON, D.L., SREENIVASAN, K.R., POPE, S.B., MENEVEAU, C. & NICHOLS, S. 2025 Small-scale properties from exascale computations of turbulence on a 32, 768^3 periodic cube. *J. Fluid Mech.* **1019**, R2.

YEUNG, P.K., SREENIVASAN, K.R. & POPE, S.B. 2018 Effects of finite spatial and temporal resolution on extreme events in direct numerical simulations of incompressible isotropic turbulence. *Phys. Rev. Fluids* **3**, 064603.